Energy spectrum and the quantum Hall effect on the square lattice with next-nearest-neighbor hopping

Y. Hatsugai and M. Kohmoto

Institute for Solid State Physics, University of Tokyo, 7-22-1 Roppongi, Minato-ku, Tokyo 106, Japan

We study the energy spectrum and the Hall effect of electrons on the square lattice with next-nearest-neighbor (NNN) hopping as well as nearest-neighbor hopping. This lattice includes the triangular lattice as a special case. We study the system under general rational values of magnetic flux per unit cell $\phi = p/q$. The structure of the secular equation is studied in detail, and the $\mathbf{k}$ dependence of the energy is analytically obtained. In the absence of NNN hopping, the two bands at the center touch for q even; thus the Hall conductance is not well defined at half-filling. An energy gap opens there by introducing NNN hopping. When $\phi = \frac{1}{2}$, the NNN model coincides with the mean-field Hamiltonian for the chiral spin state proposed by Wen, Wilczek, and Zee [Phys. Rev. B **39**, 11413 (1989)]. At half-filling for q even, the Hall conductance is calculated from the Diophantine equation and the E-ϕ diagram. We also explicitly calculate the Hall conductance for $\phi = \frac{1}{2}$ using the wave function. We find that gaps close for other fillings at certain values of NNN hopping strength. The quantized value of the Hall conductance changes once this phenomenon occurs.

I. INTRODUCTION

The problem of tight-binding electrons in two dimensions under a magnetic field is an old one (see Refs. 1–3 and references therein), and it shows extremely rich and interesting behavior. The Hamiltonian is written

$$H = - \sum_{\langle ij \rangle} t_{ij} c_j^\dagger c_i e^{i\theta_{ij}} + \text{H.c.} , \tag{1.1}$$

where c_i is the usual fermion operator at site i. The phase factor $\theta_{ij} = -\theta_{ji}$ is defined on a link $\langle i,j \rangle$. If we identify θ_{ij} as $(2\pi e/ch)\int_i^j \mathbf{A} \cdot d\mathbf{l}$, where $\mathbf{A}$ is a vector potential of the magnetic field, the quantity

$$\frac{1}{2\pi} \sum_{\text{around } S} \theta_{ij} = \frac{e}{ch} \oint_{\partial S} \mathbf{A} \cdot d\mathbf{l} = \frac{1}{\phi_0} \int_S \mathbf{B} \cdot d\mathbf{S}$$

is the magnetic flux through the area S in units of the magnetic flux quantum $\phi_0 = ch/e$. Without a magnetic field, the spectrum of tight-binding electrons on a square lattice with next-nearest (NN) hopping consists of a single band. But, when a rational magnetic flux

$$\phi = \frac{1}{2\pi} \sum_{\text{plaquette}} \theta_{ij} = \frac{p}{q}$$

(p and q being mutually prime integers) is applied, the spectrum split into q subbands. Thouless *et al.*[4] showed that each subband carries an integral Hall conductance. This is discussed by Avron *et al.*[5] using homotopy theory. The integer has a topological origin.[6] It is the Chern number of a fiber bundle which is defined by the wave functions on a two-torus: the reciprocal space (magnetic Brillouin zone) of this problem.

Recently, there has been a renewal of interest in this subject because this spectrum has been shown to have a connection with the ground-state energy of a mean-field theory of the *t-J* model.[7–9] The connection between this subject and the *t-J* model has also been studied numerically.[10,11] Several groups studied the stability of the state with respect to the magnetic field.[12–15] If the number of electrons per site ν is fixed, the total energy of the electrons has cusplike minima when the Fermi energy jumps across a gap as a function of magnetic flux ϕ, and it has an absolute minimum when $\phi = \nu$, i.e., one flux quantum per electron. This is an important and interesting result, especially in relation to the flux state and its generalization, such as the chiral spin state proposed by Wen, Wilczek, and Zee.[16]

In this paper, we study the energy spectrum and the Hall conductance of the square lattice with next-nearest-neighbor (NNN) hopping as well as nearest-neighbor hopping. This model includes the NN hopping model on the triangular lattice as a special case. The spectrum of the model with only NN hopping on the square lattice has a degeneracy at the center when q is even, i.e., the
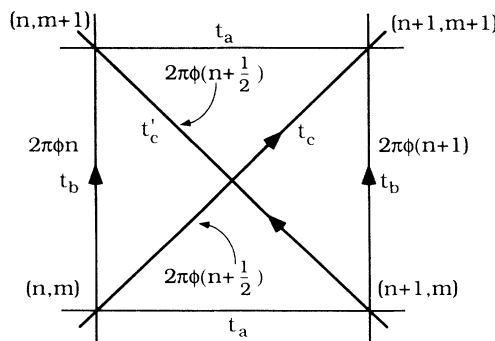

FIG. 1. The square lattice with NN hopping and NNN hopping in the magnetic field.

two central bands touch at $E=0$ (zero mode).[17,18] At this point the Hall conductance is not well defined. The NNN hopping, however, breaks this degeneracy and we obtain more insight into this degeneracy. We also find that other gaps close at certain values of the strength of NNN hopping. The quantized value of the Hall conductance changes once this phenomena occurs.

This model has another interesting relation to high-temperature superconductivity in view of the chiral state model of the Heisenberg magnet.[16] In the mean-field treatment of the chiral spin model, the Hamiltonian is equivalent to our Hamiltonian.

II. MODEL AND THE BASIC FORMULATION

We consider tight-binding electrons on a square lattice in a magnetic field with NNN hopping as well as NN hopping. The Hamiltonian is written

$$H = -t_a \sum_{n,m} c^\dagger_{n+1,m} c_{n,m} \exp(i\theta_{n+1m;nm}) - t_b \sum_{n,m} c^\dagger_{n,m+1} c_{n,m} \exp(i\theta_{nm+1;nm})$$

$$-t_c \sum_{n,m} c^\dagger_{n+1,m+1} c_{n,m} \exp(i\theta_{n+1m+1;nm}) - t'_c \sum_{n,m} c^\dagger_{n,m+1} c_{n+1,m} \exp(i\theta_{nm+1;n+1m}) + \text{H.c.} \tag{2.1}$$

The lattice spacing is taken to be unity for simplicity. For a uniform magnetic field, we take a gauge shown in Fig. 1, which gives flux ϕ for each square and flux $\phi/2$ for each triangle. When t'_c is set to zero, this lattice is topologically equivalent to the triangular lattice. We rewrite the Hamiltonian by operator $c(\mathbf{k})$ in the reciprocal space defined by

$$c_{nm} = \frac{1}{(2\pi)^2} \int_0^{2\pi} dk_x \int_0^{2\pi} dk_y \exp[i(k_x n + k_y m)] c(k_x, k_y) . \tag{2.2}$$

The result is

$$H = \frac{1}{(2\pi)^2} \int_0^{2\pi} dk_x \int_0^{2\pi} dk_y H(\mathbf{k}) , \tag{2.3}$$

$$H(\mathbf{k}) = -t_a e^{ik_x} c^\dagger(k_x, k_y) c(k_x, k_y) - t_b e^{ik_y} c^\dagger(k_x, k_y) c(k_x + 2\pi\phi, k_y)$$

$$-t_c e^{i(k_y + k_x + \pi\phi)} c^\dagger(k_x, k_y) c(k_x + 2\pi\phi, k_y) - t'_c e^{i(k_y - k_x - \pi\phi)} c^\dagger(k_x, k_y) c(k_x + 2\pi\phi, k_y) + \text{H.c.} \tag{2.4}$$

We set $k_x = k_x^0 + 2\pi\phi j$, and define

$$c_j(k_x^0, k_y) = c(k_x^0 + 2\pi\phi j, k_y) . $$

The eigenstate ψ is given by

$$\psi(k_x^0, k_y) = \sum_{j=1}^q u_j(k_x^0, k_y) c_j^\dagger(k_x^0, k_y) |0\rangle , \tag{2.5}$$

where (k_x^0, k_y) is defined in the magnetic Brillouin zone $0 \le k_x^0 \le 2\pi/q$ and $0 \le k_y \le 2\pi$. The Schrödinger equation $H\psi = E\psi$ gives

$$\tilde{B}^*_{j-1} u_{j-1} + A_j u_j + \tilde{B}_j u_{j+1} = E u_j \quad (j=1,\ldots,q) , \tag{2.6}$$

where $u_0 = u_q$, $u_1 = u_{q+1}$, and A_j and $\tilde{B}_j$ are given by

$$A_j = -2t_a \cos(k_x^0 + 2\pi\phi j) , \tag{2.7}$$

$$\tilde{B}_j = -e^{ik_y}(t_b + t_c e^{i(k_x^0 + 2\pi\phi j + \pi\phi)} + t'_c e^{-i(k_x^0 + 2\pi\phi j + \pi\phi)})$$

$$= -e^{ik_y} B_j . \tag{2.8}$$

Note that (2.6) has a duality which is a generalization of that for the NN model.[17,19] The form of (2.6) is the same under the change

$$u_j \to f_n = \sum_j e^{i2\pi\phi nj} u_j , $$

$$(k_x^0, k_y) \to (k_y, k_x^0) , \tag{2.9}$$

$$(t_a, t_b, t_c, t'_c) \to (t_b, t_a, t_c, t'_c) . $$

Let us introduce a unitary transformation $u_j = e^{ik_y j} v_j$, then (2.6) becomes

$$\det(\underline{D} - E\underline{I}) = 0 , \tag{2.10}$$

where

$$\underline{D} = \begin{bmatrix} A_1 & B_1 & \cdots & & & & B_q^* e^{-iqk_y} \\ B_1^* & A_2 & B_2 & \cdots & & & \\ & B_2^* & A_3 & B_3 & & & \\ \vdots & & \ddots & \ddots & \ddots & & \vdots \\ & & & B_{q-3}^* & A_{q-2} & B_{q-2} & \\ & & & \cdots & B_{q-2}^* & A_{q-1} & B_{q-1} \\ B_q e^{iqk_y} & & & & \cdots & B_{q-1}^* & A_q \end{bmatrix} \tag{2.11}$$

and $\underline{I}$ is the unit matrix. It is easy to see that the k_y dependence of (2.10) is

$$2(-1)^{q-1}\mathrm{Re}\,e^{iqk_y}\prod_{j=1}^{q}B_j \ , \tag{2.12}$$

and $(-1)^{q-1}\prod_{j=1}^{q}B_j$ is given in closed form as (see Appendix)

$$-t_b^q-\sum_{r=1}^{[q/2]}\frac{q}{r}\begin{bmatrix}q-r-1\\r-1\end{bmatrix}t_b^{q-2r}(t_ct_c')^r(-1)^r+(-1)^{p+q}(t_c^qe^{iqk_x^0}+t_c'^qe^{-iqk_x^0}) \ .$$

From the duality and (2.12), (2.10) becomes

$$F(E)=f(k_x^0,k_y) \ , \tag{2.13}$$

with

$$f(k_x^0,k_y)=2\cos(qk_x^0)\left[t_a^q+\sum_{r=1}^{[q/2]}(-1)^r\frac{q}{r}\begin{bmatrix}q-r-1\\r-1\end{bmatrix}t_a^{q-2r}(t_ct_c')^r\right]$$

$$+2\cos(qk_y)\left[t_b^q+\sum_{r=1}^{[q/2]}(-1)^r\frac{q}{r}\begin{bmatrix}q-r-1\\r-1\end{bmatrix}t_b^{q-2r}(t_ct_c')^r\right]$$

$$-2(-1)^{p+q}\{t_c^q\cos[q(k_x^0+k_y)]+t_c'^q\cos[q(k_x^0-k_y)]\} \ , \tag{2.14}$$

where the function $F(E)$ is a qth-order polynomial of E which does not depend on (k_x^0,k_y) (see Fig. 2).

III. SPECTRUM AND THE HALL CONDUCTANCE

A. Spectrum

We can show from (2.13) that the spectrum consists of q subbands and that these subbands do not overlap. Since (2.11) is a Hermitian matrix, all the eigenvalues are real. Thus, (2.13) has q real roots for a given value of $f(k_x^0,k_y)$. These q roots do not cross as $f(k_x^0,k_y)$ is

varied because $F(E)$ is independent of k_x^0 and k_y. This implies that the subbands do not overlap. It can happen that one has degenerate eigenvalues when $f(k_x^0,k_y)$ is at the maximum or the minimum. In this case, the two subbands touch and the gap closes.

The band edges of energy bands are given by the k points which give maximum or minimum values of $f(k_x^0,k_y)$ (see Fig. 2). An example $f(k_x^0,k_y)$ is shown in Fig. 3. (Note that the magnetic Brillouin zone is q times larger in the k_y direction.) We have calculated the energy band-flux diagram (E-ϕ diagram) using this property. The flux is taken as $\phi=p/q$, where q is the large prime integer 307 and $1\leq p\leq 306$. The E-ϕ diagram of the NN
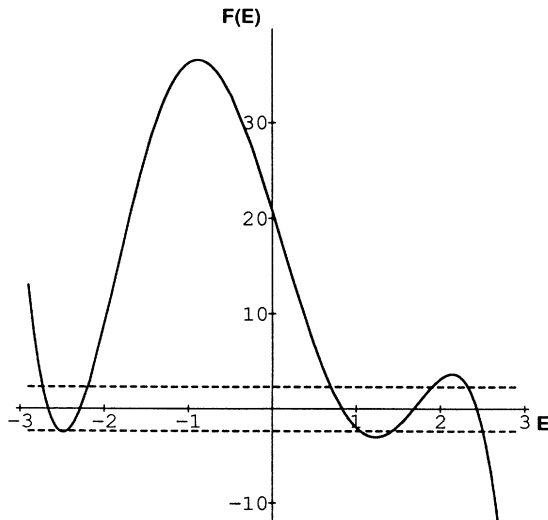

FIG. 2. An example of determining the spectrum. ($p/q=\frac{2}{5}$ and $t_a=t_b=1$, $t_c=t_c'=0.3$.) The two dashed lines represent the maximum and minimum of $f(k_x^0,k_y)$.
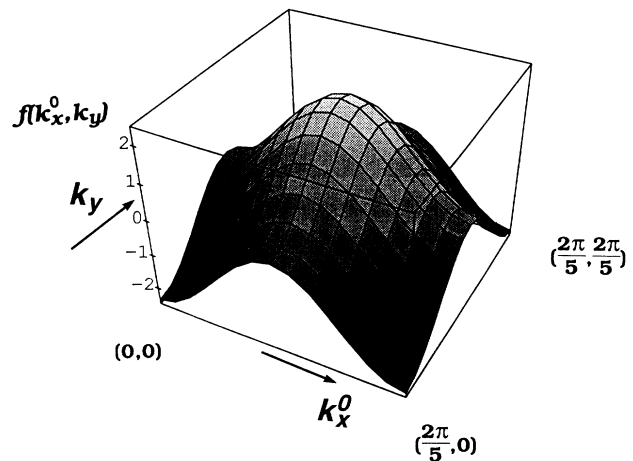

FIG. 3. $f(k_x^0,k_y)$ for $p/q=\frac{2}{5}$ and $t_a=t_b=1$, $t_c=t_c'=0.3$. The magnetic Brillouin zone is q times larger in the k_y direction and $f(k_x,k_y)$ is periodic along this direction.
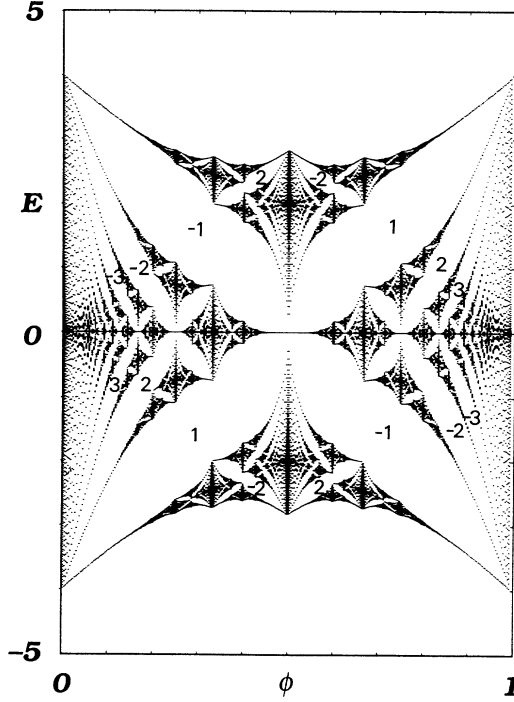
FIG. 4. The energy spectrum of the NN model for $\phi = p/307$ $(t_a = t_b = 1, t_c = t_c' = 0)$. Integers in the energy gaps are t_r.

model is shown in Fig. 4 and those of the NNN model are shown in Fig. 5. We set $t_a = t_b = 1$ and change t_c $(=t_c')$: $t_c = 0.1$ in Fig. 5(a), $t_c = -0.1$ in Fig. 5(b), and $t_c = 1$ in Fig. 5(c). It is known that there are degenerate zero modes if q is even in the NN model (see Fig. 4). Near these points, the energy dispersion is linear in $|\mathbf{k}|$.[17] In Fig. 6, we show the energy dispersion for $q = 2$. This degeneracy is removed by introducing the NNN hopping as shown by Wen, Wilczek, and Zee.[16] In Fig. 7, we show the energy dispersion for $q = 2$ with $t_c = t_c' = 0.3$. This phenomenon is not a special case of $q = 2$. We find that these degeneracies are removed by introducing the NNN hopping for general q (at least small q) in Figs. 5(a) and 5(b).

The E-ϕ diagram of the NNN model has several symmetries. (i) The spectrum is same for ϕ and $-\phi$ because the sign of the flux changes if we change the direction of the magnetic field. This invariance is also easily seen from the secular equation. (ii) The period of the diagram with respect to ϕ is 2 because the area of the fundamental triangular is $\frac{1}{2}$ and the flux through the area is $\phi/2$. (iii) If the sign of the NNN hopping is reversed, the energy is inverted at $E = 0$ [see Figs. 5(a) and 5(b)].[20] (iv) It is equivalent to increase ϕ by one and to change the sign of t_c and t_c' (see Fig. 1). Thus, the diagram is invariant, if we change ϕ to $1 + \phi$ and E to $-E$ from (iii). (v) The spectrum of the $1 - \phi$ system is obtained from that of the ϕ system by changing the sign of the energy from (i) and (iv). By the properties (i)–(v), it is sufficient to calculate the spectrum only for ϕ from 0 to $\frac{1}{2}$, which is $\frac{1}{4}$ of the period.

The spectrum for $t_a = t_b = 1$, $t_c = t_c' = 1$ is shown in Fig.

5(c). Figures 5(a) and 5(c) are topologically different. For example, the second gap at $\phi = \frac{1}{3}$ seen in Fig. 5(a) is not seen in Fig. 5(c). There is a large gap which runs from left to right in a downward slope in Fig. 5(a). However, there are only two distinct subbands in Fig. 5(c). This implies that some gaps close at a certain value of the NNN hopping strength $(t_c = t_c')$ between 0 and 1. We investigate this by the analytical expression (2.13) with (2.14) which gives the band edges. In Fig. 8, we show the band structure for (a) $\phi = \frac{1}{3}$ and (b) $\phi = \frac{1}{4}$ as a function of t_c $(=t_c')$. This shows that gaps close at several values of t_c. In fact, the zero mode of the NN model for q even is a typical example of the gap closing. At this degenerate point, the dispersion relation is linear

$$E(\mathbf{k}) \approx \pm \text{const} |\mathbf{k} - \mathbf{k}_0| + E_0 \qquad (3.1)$$

because $F(E) \approx C(E - E_0)^2$ and

$$f(k_x^0, k_y) \approx C' |\mathbf{k} - \mathbf{k}_0|^2$$

near the degenerate points where C and C' are some constants. For example, the second gap of the $\phi = \frac{1}{3}$ case closes at $t_c = t_c' \approx 0.268$ and the energy dispersion is shown in Fig. 9. The energy gap near $E \approx 1.5$ closes at $(0,0)$, $(0, 2\pi/3)$, and $(0, 4\pi/3)$ in the magnetic Brillouin zone [see also Fig. 8(a)]. The linear dispersions near these degenerate points are explicitly shown. The filling is, however, not half-filled when the Fermi energy is just at this degenerate mode. If t_c or t_c' take a slightly different value from the ones which cause degeneracies, the spectra have small energy gaps.

B. Hall conductance

Next we consider the Hall conductance of the NNN model. The contribution to the Hall conductance from a single subband is given by[4,6,17]

$$\sigma_{xy} = \frac{e^2}{h} \frac{1}{2\pi i} \int_0^{2\pi/q} dk_x^0 \int_0^{2\pi} dk_y [\nabla_\mathbf{k} \times \langle \psi(\mathbf{k}) | \nabla_\mathbf{k} | \psi(\mathbf{k}) \rangle]_z.$$

$$(3.2)$$

This formula has a subtle topological nature which is essential in the quantization of the Hall conductance. First one may naively wish to apply Stokes theorem to (3.2) to obtain

$$\sigma_{xy} = \frac{e^2}{h} \frac{1}{2\pi i} \oint_{\partial_{\text{MBZ}}} d\mathbf{k} \cdot \langle \psi(\mathbf{k}) | \nabla_\mathbf{k} | \psi(\mathbf{k}) \rangle,$$

where $\oint_{\partial_{\text{MBZ}}} d\mathbf{k}$ is a line integral around the magnetic Brillouin zone (MBZ). The magnetic Brillouin zone is topologically a two-torus and there is no boundary, that is $\partial_{\text{MBZ}} = 0$. Thus, we would have $\sigma_{xy} = 0$ in all cases. This argument, however, is not correct. The integrand $\langle \psi(\mathbf{k}) | \nabla_\mathbf{k} | \psi(\mathbf{k}) \rangle$ is written by the phase of the wave function. Assigning a phase to a state is a subtle problem. The essential point here is that the magnetic Brillouin zone is topologically a two-torus and, in general, it is not possible to define a global phase of a wave function on it. The phase of the wave function gives a principal U(1) bundle over the two-torus and $\langle \psi(\mathbf{k}) | \nabla_\mathbf{k} | \psi(\mathbf{k}) \rangle$ gives the

connection. Now the expression (3.2) represents the Chern number of the fiber bundle which is necessarily an integer. Therefore, the Hall conductance is an integer in units of e^2/h. A detailed account of this point can be found in Ref. 6.

For the NN model, if the Fermi energy lies in the rth gap from the bottom, the value of the Hall conductance, namely the sum of the contributions from the subbands which are below the Fermi energy, is given by $(e^2/h)t_r$.[17] Here t_r is the solution of the Diophantine equation

(a)

(b)

(c)
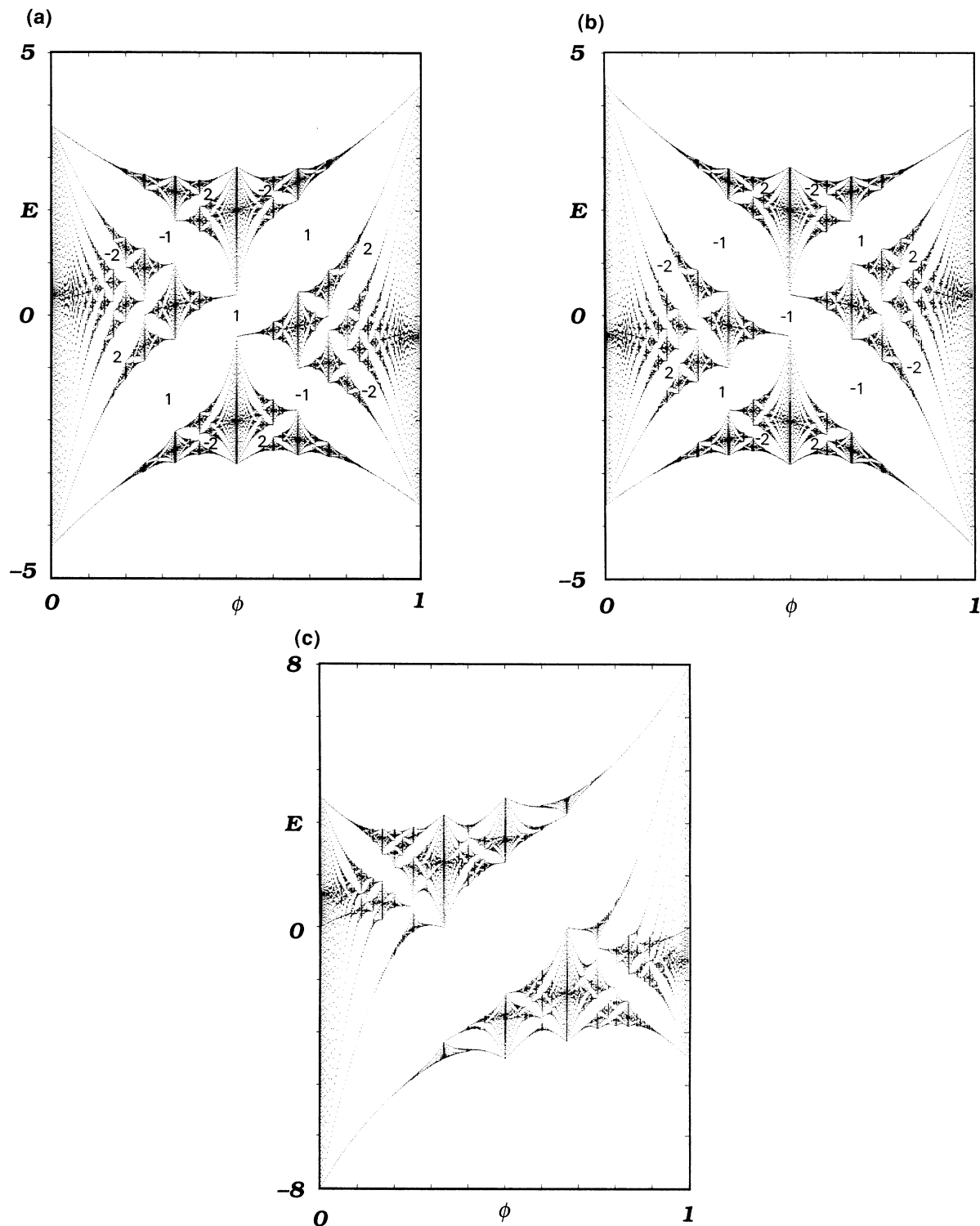
FIG. 5. The energy spectrum of the NNN model for $\phi=p/307$. The parameters are (a) $t_a=t_b=1$, $t_c=t_c'=0.1$; (b) $t_a=t_b=1$, $t_c=t_c'=-0.1$; and (c) $t_a=t_b=1$, $t_c=t_c'=1$. In (a) and (b) the integers in the energy gaps are t_r.
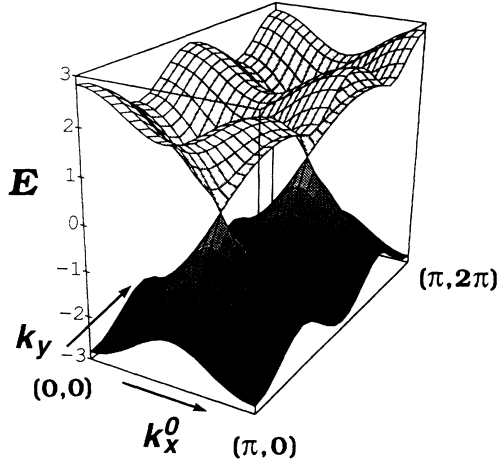
FIG. 6. The energy dispersion for $p/q = \frac{1}{2}$ and $t_a = t_b = 1$, $t_c = t'_c = 0.0$. The horizontal plane is the magnetic Brillouin zone. The existence of zero modes and the linear dispersion near these zero modes are seen.

$$r = qs_r + pt_r ,$$ (3.3)

where s_r and t_r are integers and $|t_r| \leq q/2$ and $1 \leq r \leq q$. In the NN model, t_r is shown in Fig. 4. If we fix the Fermi energy in an energy gap and change ϕ, (r,q,p) change drastically. The parameters (t_r, s_r), however, remain the same. This means that the global structure of the E-ϕ diagram determines (t_r, s_r); that is, the Hall conductance is determined by the global or topological structure of the E-ϕ diagram. At the degenerated zero modes for q even, the Diophantine equation has two solutions,

$$(t_r, s_r) = \left[\pm \frac{q}{2}, \frac{1 \mp p}{2} \right]$$

for $r = q/2$, namely, at $E = 0$. We cannot determine the
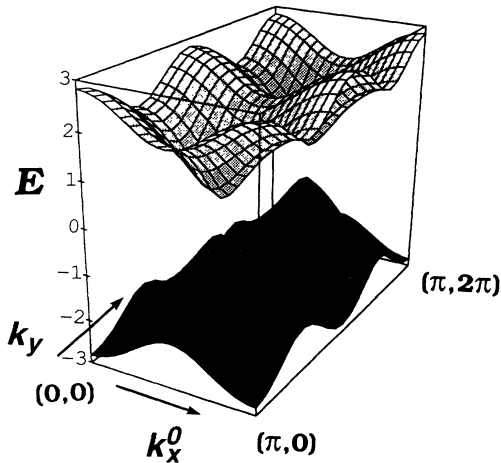

FIG. 7. Energy dispersion for $p/q = \frac{1}{2}$ and $t_a = t_b = 1$, $t_c = t'_c = 0.1$. The horizontal plane is the magnetic Brillouin zone. The degeneracy at the zero modes is removed.

Hall conductance uniquely from the Diophantine equation.

Now let us include NNN hopping. If t_c is sufficiently small, the global structure of the E-ϕ diagram is unchanged. In this case, it is possible to assign (t_r, s_r) to large gaps from those of the NN model. Thus, we can get a Hall conductance of the NNN model from its E-ϕ diagram. At the zero modes in the NN model, the degeneracy is removed and gaps open by introducing NNN hopping. Once the degeneracies are removed, we can assign the Hall conductance by the global structure of the E-ϕ diagram. We show t_r in Fig. 5(a). This shows that the degeneracy at half-filled case, that is, $r = q/2$ in $\phi = 1/q$ (q: even), is removed and the Hall conductance corresponding to these gaps is $+q/2$ for $t_c = t'_c > 0$ (at least for $q = 2, 4, 6, 8$). When $t_c = t'_c < 0$, the Hall conductance is $-q/2$ by the symmetry of the E-ϕ diagram.

We investigate the Hall conductance when the gap-closing phenomenon occurs.[21] The Hall conductance is determined by the global structure of the E-ϕ diagram. If the gap-closing phenomenon occurs, the topological structure of the E-ϕ diagram changes and the Hall conductance of the systems also changes. The energy gaps of the NN model are all labeled by the t_r and s_r by the Diophantine equation. If the gap closes, the correspond-
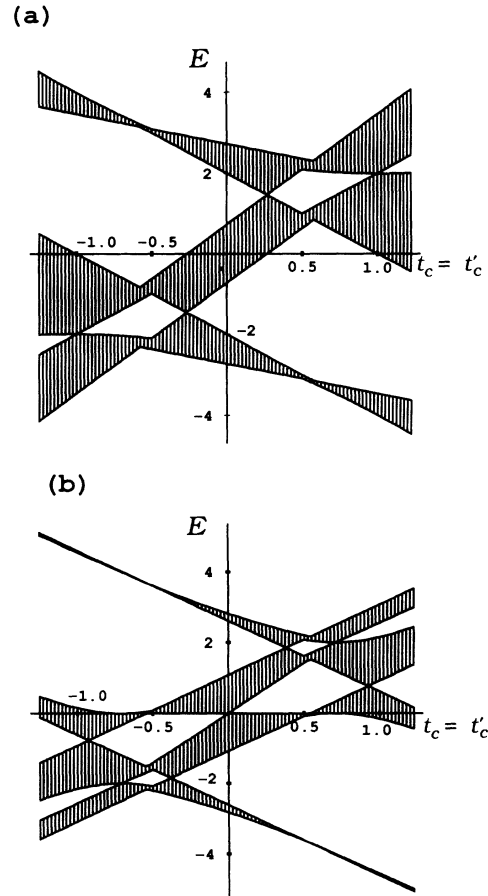
(a)

(b)

FIG. 8. Band structure of the NNN model as a function of the NNN hopping t_c $(= t'_c)$ for (a) $\phi = \frac{1}{3}$ and (b) $\phi = \frac{1}{4}$.
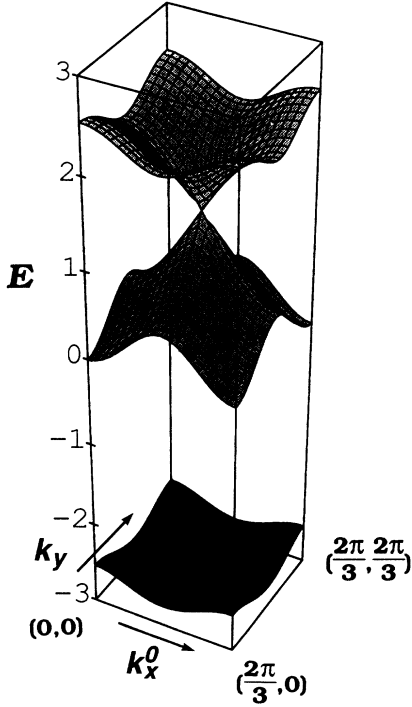
FIG. 9. Energy dispersion for $p/q = \frac{1}{3}$ and $t_a = t_b = 1$, $t_c = t_c' = 0.268$. The magnetic Brillouin zone is three times larger along the k_y direction, but the energy dispersion is periodic along this direction. This shows that there are degenerated modes and near these points dispersion is linear similar to the $\frac{1}{2}$ case in the NN model. The integers in the energy gaps are t_r.

ing t_r and s_r change. We cannot determine (t_r, s_r) at a special value of the flux if the gap closes once. However, the global structure of the E-ϕ diagram is not changed except near the degenerate point (where the gap closes) by small change of the NNN hopping. If we make a small enough change of the NNN hopping, the global gap structure which determines the labeling (t_r, s_r) and the Hall conductance does not change. If we increase the NNN hopping and investigate the gap-closing phenomenon and E-ϕ diagram carefully, we can always identify the (t_r, s_r) for all values of the NNN hopping. For example, we investigate the $\phi = \frac{1}{3}$ system with $\frac{2}{3}$ filling. In Figs. 10(a) and 10(b), we show the E-ϕ diagram for $t_c = t_c' = 0.2$ and $t_c = t_c' = 0.3$ The gap closes near $t_c = t_c' \approx 0.268$; however, we can assign (t_r, s_r); that is, the Hall conductance is changed from $-e^2/h$ to $2(e^2/h)$. The discontinuity of the Hall conductance Δt_r is supposed to be the integer times q from the Diophantine equation since we expect that the condition

$$r = qs_r + pt_r = qs_r' + pt_r' \qquad (3.4)$$

still holds when the degeneracy occurs, where (t_r, s_r) is the label of the gap before the gap closes and (t_r', s_r') is the one after the gap-closing phenomenon occurs. We have to notice that the t_r' does not satisfy the condition
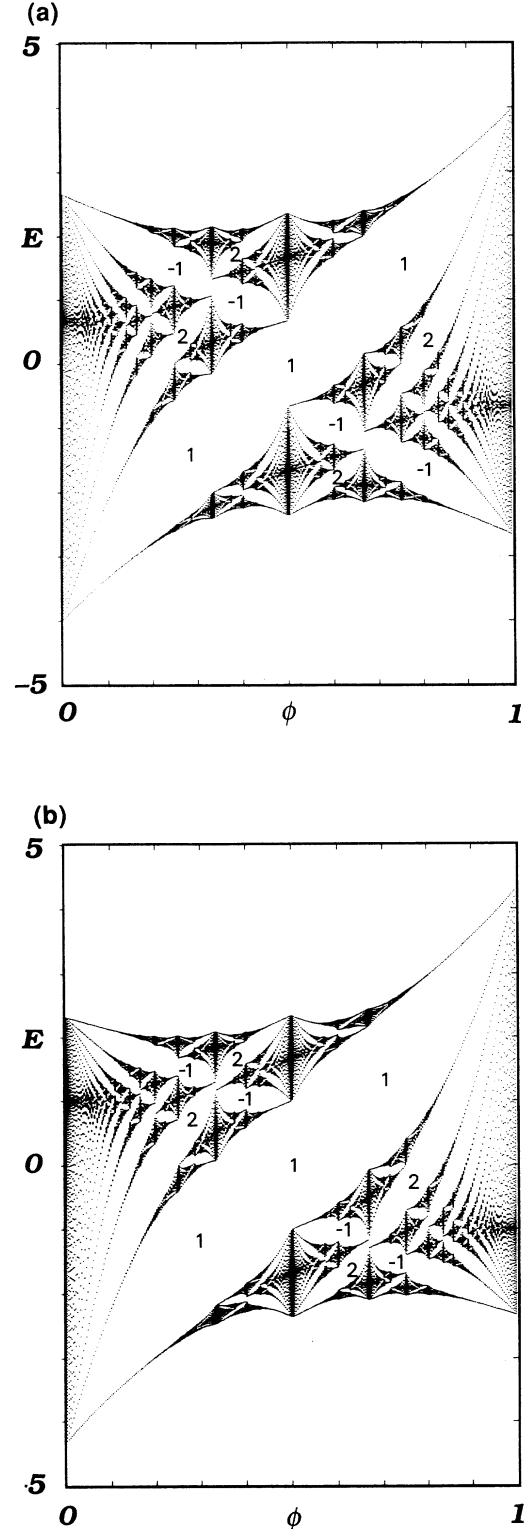

FIG. 10. The energy spectrum of the NNN model for $\phi = p/307$. The parameters are (a) $t_a = t_b = 1$, $t_c = t_c' = 0.2$ and (b) $t_a = t_b = 1$, $t_c = t_c' = 0.3$, which are slightly smaller or larger than the value at which the second gap of $\phi = \frac{1}{3}$ closes. The integers in the energy gaps are t_r.
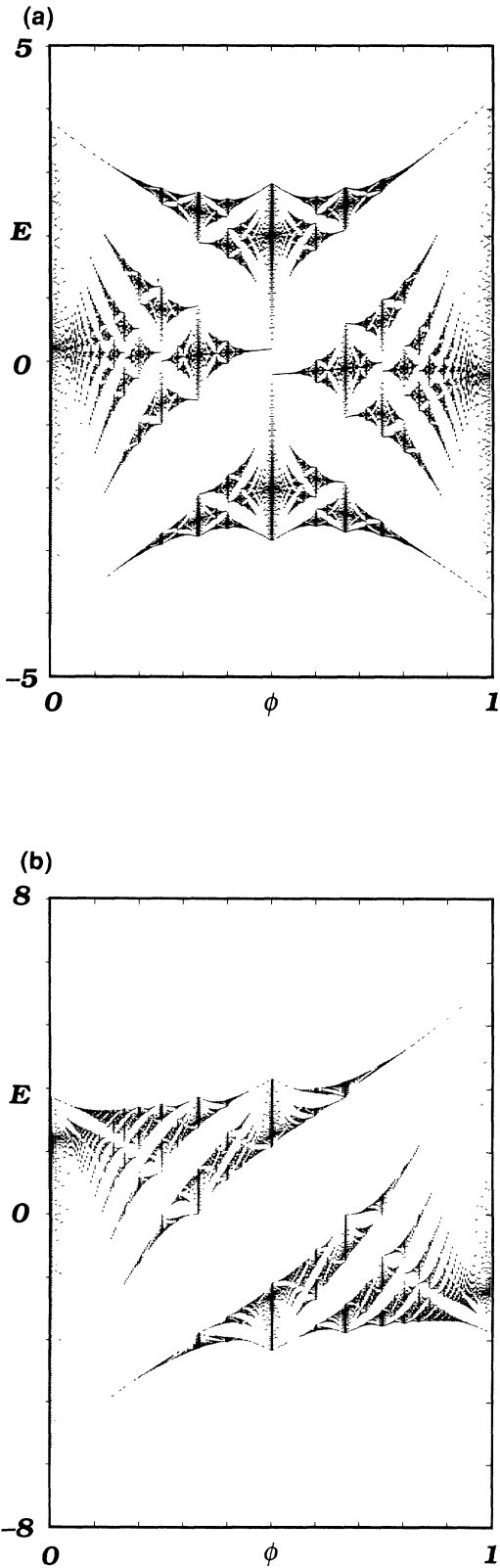
(a)

(b)

FIG. 11. The energy spectrum of the triangular lattice for $\phi = p/307$. The parameters are (a) $t_a = t_b = 1$, $t_c = t_c' = 0.1$ and (b) $t_a = t_b = 1$, $t_c = t_c' = 1$.

$|t_r| \leq q/2$. In the previous example shown in Fig. 10, (3.4) is

$$2 = (3)(1) + 1(-1) = (3)(0) + (1)(2)$$

and $t_r' = 2$ is not smaller than $\frac{3}{2}$. The contribution for this change Δt_r is brought about from the subband which is just below the Fermi energy because the contributions from the other subbands do not change. We assume that before the gap closing, the band just below the gap contributes $\tilde{t}_r$ to t_r and the band just above would contribute $\tilde{t}_{r+1}$ if the Fermi energy is above this band (that is, $t_r = \sum_{i=1}^{r} \tilde{t}_i$) and these values are changed to $\tilde{t}_r'$ and $\tilde{t}_{r+1}'$ after the gap closing. In this case, the sum of the $\tilde{t}_r + \tilde{t}_{r+1}$ is unchanged because the gap just above the gap which closes is stable and t_{r+1} does not change. This implies the conservation law

$$\tilde{t}_r + \tilde{t}_{r+1} = \tilde{t}_r' + \tilde{t}_{r+1}' , \tag{3.5}$$

which is first discussed by Avron, Seiler, and Simon.[5] In the example discussed above, (3.5) is $(-2) + (1) = (1) + (-2)$.
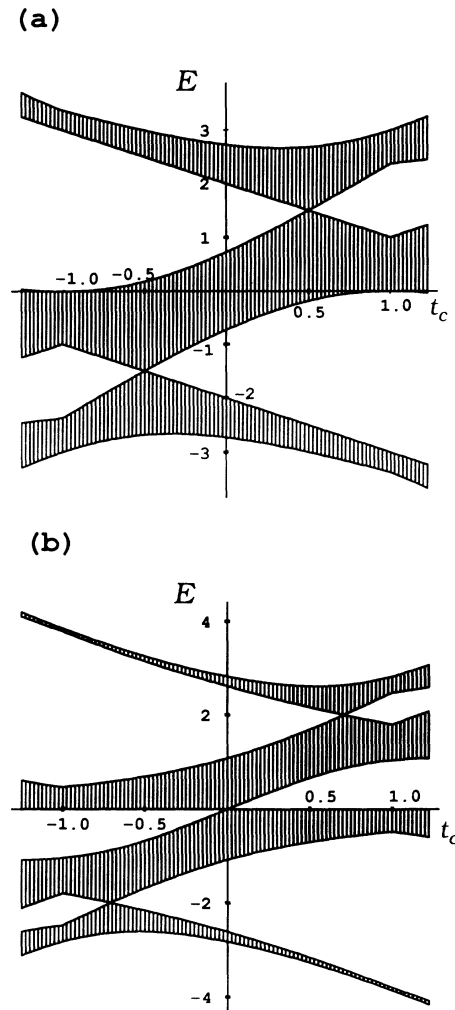
(a)

(b)

FIG. 12. The band structure of the triangular lattice as a function of the NNN hopping t_c ($t_c' = 0$) for (a) $\phi = \frac{1}{3}$ and (b) $\phi = \frac{1}{4}$.

IV. TRIANGULAR LATTICE

If t_c' (or t_c) is set to zero, the lattice shown in Fig. 1 is topologically equivalent to the triangular lattice. The spectrum for the triangular lattice was studied by Claro and Wannier[22] and the Hall conductance was discussed by Thouless.[23]

From (2.13) and (2.14), the secular equation is given by $F(E)=f(k_x^0,k_y)$ with

$$f(k_x^0,k_y)=2t_a^q\cos(qk_x^0)+2t_b^q\cos(qk_y)$$
$$-2(-1)^{p+q}t_c^q\cos[q(k_x^0+k_y)] \ . \tag{4.1}$$

From (4.1), we can determine the band edges of the spectrum. The E-ϕ diagrams for $q=307$ are shown in Fig. 11(a) for $t_a=t_b=1$, $t_c=0.1$ and in Fig. 11(b) for $t_a=t_b=1$, $t_c=1$. If t_c is sufficiently small, the gaps in the

NN model do not close and one can assign (t_r,s_r) at each gap by the Diophantine equation (3.3) and this gives the Hall conductance. In Fig. 12, we show the behavior of the band for (a) $\phi=\frac{1}{3}$ and (b) $\phi=\frac{1}{4}$ as a function of t_c. The topological structure of the E-ϕ diagram changes when we increase t_c from 0 to 1. Gap-closing phenomena occur and the Hall conductance changes in a similar manner to the NNN model. However, we can assign the Hall conductance for the $t_c=1$ case by investigating the E-ϕ diagram in detail as performed in the last section.

V. EXPLICIT CALCULATION OF THE HALL CONDUCTANCE FOR $\phi=\frac{1}{2}$

We calculate the Hall conductance at half-filling for $\phi=\frac{1}{2}$ with nonzero t_c+t_c' and $t_a>0$. In this case, we have a 2×2 matrix eigenvalue problem given by

$$\mathbf{H}(\mathbf{k})\begin{bmatrix} a \\ b \end{bmatrix}=E\begin{bmatrix} a \\ b \end{bmatrix} \ , \tag{5.1}$$

$$\mathbf{H}(\mathbf{k})=\begin{bmatrix} A(\mathbf{k}) & B(\mathbf{k}) \\ B^*(\mathbf{k}) & -A(\mathbf{k}) \end{bmatrix} \ , \tag{5.2}$$

$$A(\mathbf{k})=-2t_a\cos(k_x^0) \ , \tag{5.3}$$

$$B(\mathbf{k})=\tilde{B}_0+\tilde{B}_1^*$$
$$=-e^{ik_y}(t_b+t_ce^{i(k_x^0+\pi/2)}+t_c'e^{-i(k_x^0+\pi/2)})-e^{-ik_y}(t_b+t_ce^{-i(k_x^0+\pi+\pi/2)}+t_c'e^{i(k_x^0+\pi+\pi/2)})$$
$$=-e^{ik_y}(t_b+it_ce^{ik_x^0}-it_c'e^{-k_x^0})-e^{-ik_y}(t_b+it_ce^{-ik_x^0}-it_c'e^{ik_x^0})$$
$$=-2t_b\cos(k_y)-i2[t_c\cos(k_x^0+k_y)-t_c'\cos(k_x^0-k_y)] \ . \tag{5.4}$$

The energies are

$$E(\mathbf{k})=E_\pm(\mathbf{k})$$
$$=\pm[A^2(\mathbf{k})+B'^2(\mathbf{k})]^{1/2}$$
$$=\pm2t_a\left[\cos^2(k_x^0)+\left[\frac{t_b}{t_a}\right]^2\cos^2(k_y)+\left[\frac{t_c}{t_a}\cos(k_x^0+k_y)-\frac{t_c'}{t_a}\cos(k_x^0-k_y)\right]^2\right]^{1/2} \ , \tag{5.5}$$

where $B'(\mathbf{k})$ is real and is defined by

$$B(\mathbf{k})=B'(\mathbf{k})\exp[i\zeta(\mathbf{k})] \ , \tag{5.6}$$

where the phase factor $\zeta(\mathbf{k})$ is chosen to be 0 at $k_x^0=k_y=0$. In this section, we take a magnetic Brillouin zone as $-\pi/2\le k_x^0\le\pi/2$ and $0\le k_y\le2\pi$. See Fig. 13.

For a half-filled case, the lower band (E_-) is filled. To get the wave function, we need to choose a phase convention. It does not matter if we choose a different convention at each $\mathbf{k}$ point and it is related to the local ($\mathbf{k}$-dependent) gauge freedom.[6] Here we calculate σ_{xy} by two different gauges: a is always real and b is always real.

First we take a gauge where a is always real. Let us set

$$b=b'\exp[-i\zeta(\mathbf{k})] \ , \tag{5.7}$$

and the wave function, which gives the energy E_-, is written

$$\begin{bmatrix} a(\mathbf{k}) \\ b'(\mathbf{k}) \end{bmatrix}=\begin{bmatrix} -\sin\theta(\mathbf{k}) \\ \cos\theta(\mathbf{k}) \end{bmatrix} \ , \tag{5.8}$$

where $\theta(\mathbf{k})$ is chosen as

$$\cos[2\theta(\mathbf{k})]=\frac{A(\mathbf{k})}{[A^2(\mathbf{k})+B'^2(\mathbf{k})]^{1/2}} \ ,$$
$$\sin[2\theta(\mathbf{k})]=\frac{B'(\mathbf{k})}{[A^2(\mathbf{k})+B'^2(\mathbf{k})]^{1/2}} \ . \tag{5.9}$$

If we calculate σ_{xy} by dividing the magnetic Brillouin zone to several patches Δ_i, the expression for σ_{xy} is

$$\sigma_{xy}=\frac{e^2}{h}\frac{1}{2\pi i}\sum_{\Delta_i}\oint_{\partial\Delta_i}d\mathbf{k}\cdot[a^*(\mathbf{k}),b^*(\mathbf{k})]\nabla_\mathbf{k}\begin{bmatrix} a(\mathbf{k}) \\ b(\mathbf{k}) \end{bmatrix} \ . \tag{5.10}$$
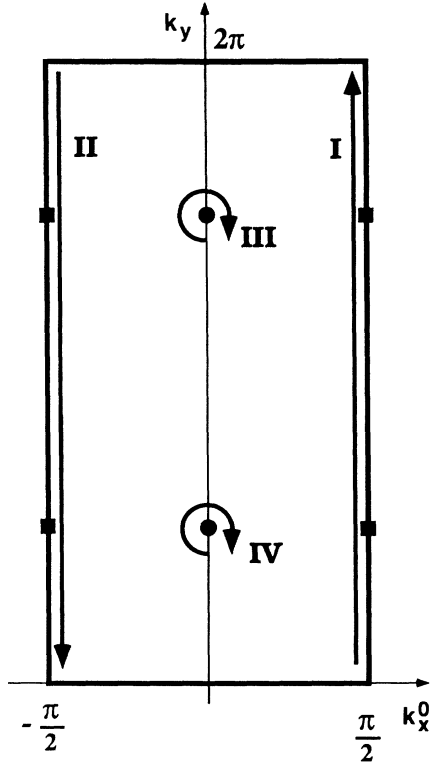
FIG. 13. The path of the integration for calculating σ_{xy} in the magnetic Brillouin zone for $\phi = \frac{1}{2}$.

As a result, it is necessary to include the following four integrals shown in Fig. 13. The solid circles at III and IV are points where $B(\mathbf{k})$ or $B'(\mathbf{k})$ is zero and a phase of $B(\mathbf{k}), \zeta(\mathbf{k})$ is not defined. The solid squares are the highest-energy points where the degeneracy takes place if $t_c + t'_c$ is zero. The contribution from I and II is due to the fiber-bundle character of the problem; that is, these two lines are equivalent in the magnetic Brillouin zone but the phases are not defined by a global convention. This is more easily seen by dividing the magnetic Brillouin zone by two patches, which are separated by lines $k_x = -\pi/2, 0$ and $\pi/2$. The integrand of (5.10) is written

$$-ib'(\mathbf{k})^2 \nabla_{\mathbf{k}} \zeta(\mathbf{k}) . \tag{5.11}$$

In regions I–IV, $b'(\mathbf{k})^2$'s take constant values:

$$b'(\mathbf{k})^2 = \tfrac{1}{2}(\mathrm{I}), \tfrac{1}{2}(\mathrm{II}), 0(\mathrm{III}), 0(\mathrm{IV}) , \tag{5.12}$$

so we can factor out the $b'(\mathbf{k})^2$ from the integrand in (5.10) and it is sufficient to investigate the change of $\zeta(\mathbf{k})$. In region I,

$$B(\mathbf{k}) = -2t_b \cos(k_y) + i2(t_c + t'_c)\sin(k_y)$$

and we have

$$\int_{\mathrm{I}} d\mathbf{k} \cdot \nabla_{\mathbf{k}} \zeta(\mathbf{k}) = -2\pi\, \mathrm{sgn}[t_b(t_c + t'_c)] . \tag{5.13}$$

In region II,

$$B(\mathbf{k}) = -2t_b \cos(k_y) - i2(t_c + t'_c)\sin(k_y)$$

and we have

$$\int_{\mathrm{II}} d\mathbf{k} \cdot \nabla_{\mathbf{k}} \zeta(\mathbf{k}) = -2\pi\, \mathrm{sgn}[t_b(t_c + t'_c)] . \tag{5.14}$$

The contributions from regions III and IV are zero in this gauge because the weight $b'(\mathbf{k})^2$ is zero at III and IV. From (5.10)–(5.14), the Hall conductance in this gauge is

$$\sigma_{xy} = \frac{e^2}{h} \frac{1}{2\pi i}(-i)(\tfrac{1}{2})\{2(-2\pi)\mathrm{sgn}[t_b(t_c + t'_c)]\}_{(\mathrm{I},\mathrm{II})}$$

$$= \frac{e^2}{h} \mathrm{sgn}[t_b(t_c + t'_c)] . \tag{5.15}$$

This result is consistent with that of Sec. III.

In another gauge where b is always real, we set

$$a = a'\exp[i\zeta(\mathbf{k})] . \tag{5.16}$$

The wave function is

$$\begin{bmatrix} a'(\mathbf{k}) \\ b(\mathbf{k}) \end{bmatrix} = \begin{bmatrix} -\sin\theta(\mathbf{k}) \\ \cos\theta(\mathbf{k}) \end{bmatrix} , \tag{5.17}$$

where the definition of $\theta(\mathbf{k})$ is the same as the previous case, that is (5.9). The integrand of (5.10) is written as

$$ia'(\mathbf{k})^2 \nabla_{\mathbf{k}} \zeta(\mathbf{k}) . \tag{5.18}$$

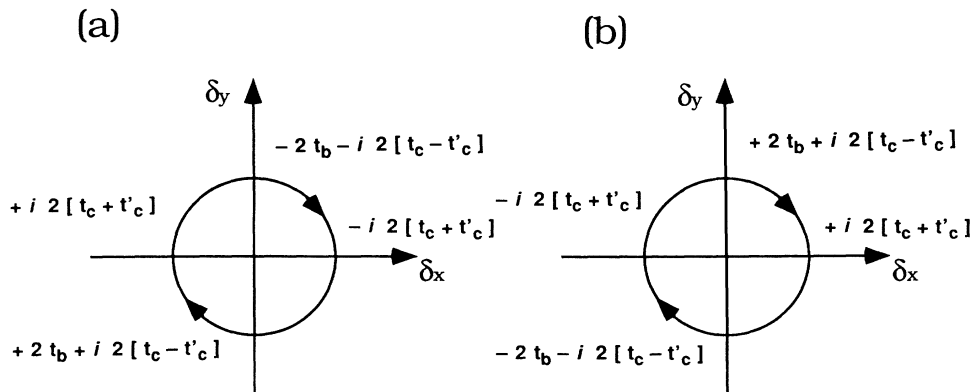$a'(\mathbf{k})^2$ is also constant at each region I–IV and takes the following values:

(a)

(b)

FIG. 14. Function $\zeta(k)$ near (a) III and (b) IV.

$$a'(\mathbf{k})^2 = \tfrac{1}{2}(\mathrm{I}), \tfrac{1}{2}(\mathrm{II}), 1(\mathrm{III}), 1(\mathrm{IV}) . \tag{5.19}$$

We can use results for I and II (5.13) and (5.14) and it is necessary to calculate a contribution from regions III and IV.

Near region III, we can set $k_x = \delta x$ and $k_y = 3\pi/2 + \delta y$ for $\delta x, \delta y \ll 1$. Then

$$B(\mathbf{k}) \approx -2t_b \delta_y - i2[(t_c + t_c')\delta x + (t_c - t_c')\delta y]$$

[see Fig. 14(a)] and we have

$$\int_{\mathrm{III}} d\mathbf{k} \cdot \nabla_{\mathbf{k}} \zeta(\mathbf{k}) = 2\pi \, \mathrm{sgn}[t_b(t_c + t_c')] . \tag{5.20}$$

Near region IV, we can set $k_x = \delta x$ and $k_y = \pi/2 + \delta y$ for $\delta x, \delta y \ll 1$. Then

$$B(\mathbf{k}) \approx +2t_b \delta y + i2[(t_c + t_c')\delta x + (t_c - t_c')\delta y]$$

[see Fig. 14(b)] and we have

$$\int_{\mathrm{IV}} d\mathbf{k} \cdot \nabla_{\mathbf{k}} \zeta(\mathbf{k}) = 2\pi \, \mathrm{sgn}[t_b(t_c + t_c')] . \tag{5.21}$$

Then the Hall conductance is calculated as

$$
\begin{aligned}
\sigma_{xy} = {} & \frac{e^2}{h} \frac{1}{2\pi i} (i(\tfrac{1}{2})\{2(-2\pi)\mathrm{sgn}[t_b(t_c + t_c')]\}_{(\mathrm{I},\mathrm{II})} \\
& + i(1)\{2(+2\pi)\mathrm{sgn}[t_b(t_c + t_c')]\}_{(\mathrm{III},\mathrm{IV})}) \\
= {} & \frac{e^2}{h} \mathrm{sgn}[t_b(t_c + t_c')] .
\end{aligned}
\tag{5.22}
$$

Thus, we obtained the same result from the two different gauges.

VI. SUMMARY AND DISCUSSIONS

We studied the energy spectrum and the Hall effect of two-dimensional electrons on the square lattice with next-nearest-neighbor hopping. In Sec. II, the structure of the secular equation was studied in detail and the $\mathbf{k}$ (in the magnetic Brillouin zone) dependence of the energy is analytically obtained. In Sec. III, we numerically studied the spectrum of the NNN model. Using the results of Sec. II, the exact band edges were obtained. The NNN model includes a mean-field Hamiltonian of the chiral spin state proposed by Wen, Wilczek, and Zee (WWZ).[16] In our notation, the chiral spin state corresponds to $\phi = \tfrac{1}{2}$ at half-filling ($r = q/2$). In the nearest-neighbor model, there are degenerate zero modes for even q.[17,18] At the zero modes, we have two solutions $t_r = \pm q/2$ of the Diophantine equation and we cannot decide the quantized Hall conductance uniquely. In fact, this point is a topological singularity on the two-dimensional energy dispersion. Since the two bands are degenerate, we do not have regular manifolds there. This degeneracy is removed for general even q by introducing NNN hopping. We observed this by numerical calculations (at least for small integer q and $p = 1$). The Hall conductance of the NNN model is studied in relation to the NN model when the Fermi energy is in an energy gap. The symmetry of the E-ϕ diagram was considered. The Hall conductance for even q flux near half-filling can be determined by the E-ϕ diagram. By the global structure of the E-ϕ diagram, we can assign the Hall conductance using the rigid topo-

logical property of the Hall conductance. With NNN hopping, a gap-closing phenomenon occurs; that is, there are degeneracies at certain values of the NNN hopping. A typical example is $\phi = \tfrac{1}{2}$ with the $t_c = t_c' = 0$ case. At the general NNN hopping where the gap-closing phenomenon happens, the energy dispersion is linear in the k space. If the NNN hopping is just away from the gap-closing value, there is a small energy gap near edges of the energy bands. The $\phi = \tfrac{1}{2}$ case discovered by WWZ is not a special case and such a situation always happens when the gap-closing phenomenon happens at finite values of NNN hopping strength.

The triangular lattice is a special case of the NNN model and we analytically obtained the $\mathbf{k}$ dependence of the energy. We have investigated the system by changing one of the three independent transfers. The degeneracies in the NN model with q even is also removed and the gap-closing phenomenon also happens. The qualitative properties are similar to the NNN model.

In Sec. V, we calculate the Hall conductance of the NNN model for $\phi = \tfrac{1}{2}$ explicitly. The fiber-bundle character of the phase of the wave function in the magnetic Brillouin zone is explicitly demonstrated. We have to divide the magnetic Brillouin zone into two pieces to calculate the Hall conductance. The mismatch at the boundary of the pieces and the vortexlike singularities give contributions to the Hall conductance. We show calculations using two different gauges. The results are consistent with the numerical treatment of Sec. III.

In view of the chiral state model, this NNN model has an interesting property. The chiral spin state is proposed for the model of the Heisenberg antiferromagnet in two dimensions. This model is approximately obtained by a second-order perturbation as to U/t (Coulomb interaction) of the usual Hubbard model. In the chiral spin state, there is no movable carrier. The energy to make an electron hop is infinity (order of U) in the chiral spin state (in the insulator this cost is the order of the energy gap) and the hopping process is prohibited. The Hall current is dissipationless and the Hall conductance of insulator, where the Fermi energy is in the band gap, is nonzero and takes a quantized value. In contrast, the Hall conductance of the chiral spin state is exactly zero due to the absence of carriers as noted by WWZ by a different argument, that is, there is no zero-field Hall effect in the chiral spin state. In a simple mean-field treatment of the chiral state, the mean-field Hamiltonian is the same as our NNN model. However, the effect of the constraint, that is, there is only one electron on each site, is not included in it. In this sense, we do not expect the Hall conductance of the NNN model is that of the zero-field Hall effect in the chiral spin state.

At last, we want to interpret the gap-closing phenomenon discussed in Sec. III in the mean-field treatment of the chiral spin state. The simplest case is the small NNN hopping model with $\phi = \tfrac{1}{2}$. The chiral spin state, that is, small t_c and t_c' with p/q being $\tfrac{1}{2}$ is not a unique case, whose dispersion relation is approximately described by the Dirac equation. Similar situations always happen when a gap closes. The filling is generally different from half-filling and the corresponding flux is

not $\frac{1}{2}$. If we extend the discussion of WWZ to a non-half-filled case, we can get a similar Chern-Simons gauge theory at a certain value of the NNN hopping where the gap closes. If we integrate out a fermion degree of freedom, we get an effective Chern-Simons Lagrangian by the standard procedure.[16] The coefficient of the Chern-Simons term, which is relevant to the statistics of the particles which couples to the virtual gauge field, is given by the Hall conductance of our NNN model. If we follow the argument of WWZ, the statistics of the quasiparticles is not always half-fermion and depends on the conditions at which the degeneracy occurs; that is, depends on the filling and the NNN hopping (strength of the mean field).

ACKNOWLEDGMENTS

APPENDIX

We want to calculate

$$-[X^q+Y^q-(-t_c)^q e^{iq(\pi\phi^+ k_x^0)}-(-t_c')^q e^{-iq(\pi\phi+k_x^0)}]=-(X^q+Y^q)+(-1)^{p+q}(t_c^q e^{iqk_x^0}+t_c'^q e^{-iqk_x^0}) \ . \tag{A6}$$

In the following we write X^q+Y^q with

$$a\equiv X+Y=t_b \ ,$$
$$b\equiv XY=t_c t_c' \ . \tag{A7}$$

X and Y are given by a and b by

$$\begin{bmatrix} X \\ Y \end{bmatrix}=\tfrac{1}{2}[a\pm(a^2-4b)^{1/2}] \ , \tag{A8}$$

and X^q+Y^q is written by a binomial expansion

$$\begin{aligned} X^q+Y^q &=\frac{1}{2^q}\sum_{k=0}^{[q/2]}\begin{bmatrix} q \\ 2k \end{bmatrix}2a^{q-2k}(a^2-4b)^k \\ &=\frac{1}{2^{q-1}}\sum_{k=0}^{[q/2]}\sum_{r=0}^{k}\begin{bmatrix} q \\ 2k \end{bmatrix}\begin{bmatrix} k \\ r \end{bmatrix}a^{q-2r}b^r 2^{2r}(-1)^r \\ &=\frac{1}{2^{q-1}}\sum_{r=0}^{[q/2]}\left[\sum_{k=r}^{[q/2]}\begin{bmatrix} q \\ 2k \end{bmatrix}\begin{bmatrix} k \\ r \end{bmatrix}\right]a^{q-2r}b^r 2^{2r}(-1)^r \ . \end{aligned} \tag{A9}$$

$$(-1)^{q-1}\prod_{j=1}^{q} B_j=-\prod_{j=1}^{q}(t_b+t_c e^{i(2\pi\phi j+\alpha)}+t_c' e^{-i(2\pi\phi j+\alpha)}) \ , \tag{A1}$$

$$\alpha=k_x^0+\pi\phi \ . \tag{A2}$$

It is easy to show

$$\prod_{j=1}^{q}(x^2+yz-xye^{i(2\pi\phi j+\alpha)}-xze^{-i(2\pi\phi j+\alpha)})$$
$$=x^{2q}+(yz)^q-x^q y^q e^{iq\alpha}-x^q z^q e^{-iq\alpha} \ . \tag{A3}$$

If we identify

$$t_b=x^2+yz, \quad t_c=-xy, \quad t_c'=-xz \ , \tag{A4}$$

and set

$$X=x^2, \quad Y=yz=\frac{t_c t_c'}{X} \ , \tag{A5}$$

the right-hand side of (A1) becomes

The quantity in the large bracket is written in a closed form (it can be proven by induction),

$$\sum_{k=r}^{[q/2]}\begin{bmatrix} q \\ 2k \end{bmatrix}\begin{bmatrix} k \\ r \end{bmatrix}=\begin{cases} \dfrac{q}{r}\begin{bmatrix} q-r-1 \\ r-1 \end{bmatrix}2^{q-2r-1} & (r\neq 0) \\ 2^{q-1} & (r=0) \ . \end{cases} \tag{A10}$$

As a result, we get the close form for X^q+Y^q as

$$X^q+Y^q=a^q+\sum_{r=1}^{[q/2]}\frac{q}{r}\begin{bmatrix} q-r-1 \\ r-1 \end{bmatrix}a^{q-2r}b^r(-1)^r \ . \tag{A11}$$

Combining (A1), (A6), and (A11), we get the result

$$\begin{aligned} (-1)^{q-1}\prod_{j=1}^{q}B_j=&-t_b^q-\sum_{r=1}^{[q/2]}\frac{q}{r}\begin{bmatrix} q-r-1 \\ r-1 \end{bmatrix} \\ &\times t_b^{q-2r}(t_c t_c')^r(-1)^r \\ &+(-1)^{p+q}(t_c^q e^{iqk_x^0}+t_c'^q e^{-iqk_x^0}) \ . \end{aligned} \tag{A12}$$

---

[1] M. Ya Azbel, Zh. Eksp. Teor. Fiz. **46**, 929 (1964) [Sov. Phys.—JETP **19**, 634 (1964)].
[2] D. R. Hofstadter, Phys. Rev. B **14**, 2239 (1976).
[3] G. H. Wannier, Phys. Status Solidi B **88**, 757 (1978); G. H. Wannier, G. M. Obermaier, and R. Ray, *ibid.* B **93**, 337 (1979).
[4] D. J. Thouless, M. Kohmoto, P. Nightingale, and M. Den Nijs, Phys. Rev. Lett. **49**, 405 (1982).

[5]J. Avron, R. Seiler, and B. Simon, Phys. Rev. Lett. **51**, 51 (1983).

[6]M. Kohmoto, Ann. Phys. (N.Y.) **160**, 355 (1985).

[7]P. W. Anderson Phys. Scr. T **27**, 60 (1989); P. W. Anderson, B. S. Shastry, and D. Hristopulos, Phys. Rev. B **40**, 8939 (1989).

[8]P. Lederer, D. Poilblanc, and T. M. Rice, Phys. Rev. Lett. **63**, 1519 (1989).

[9]J. R. Rodriguez and B. Doucot, Europhys. Lett. **11**, 451 (1990).

[10]D. Poilblanc, Y. Hasegawa, and T. M. Rice, Phys. Rev. B **41**, 1949 (1990).

[11]S. Liang and N. Trived, Phys. Rev. Lett. **64**, 232 (1990).

[12]Y. Hasegawa, P. Lederer, T. M. Rice, and P. B. Wiegmann, Phys. Rev. Lett. **63**, 907 (1989); G. Montambaux, *ibid.* **63**, 1657 (1989).

[13]M. Kohmoto and Y. Hatsugai, Phys. Rev. B **41**, 9527 (1990); Y. Hasegawa, Y. Hatsugai, M. Kohmoto, and G. Montambaux, *ibid.* **41**, 9174 (1990).

[14]D. Peter, M. Cyrot, D. Mayou, and S. N. Khanna, Phys. Rev. B **40**, 9382 (1989).

[15]F. Nori, E. Abrahams, and G. T. Zimanyi, Phys. Rev. B **41**, 7277 (1990).

[16]X. G. Wen, F. Wilczek, and A. Zee, Phys. Rev. B **39**, 11 413 (1989).

[17]M. Kohmoto, Phys. Rev. B **39**, 11 943 (1989).

[18]S. G. Wen and A. Zee, Nucl. Phys. **B316**, 641 (1989).

[19]S. Aubry and G. André, Ann. Isr. Phys. Soc. **3**, 133 (1980).

[20]First we perform a canonical transformation $c_j^\dagger \to (-1)^{P_j} c_j^\dagger$, where P_j is 1 if j is on the A sublattice and 0 if j is on the B sublattice (the square lattice is bipartite and we divide it into two sublattices A and B). Then t_a and t_b change sign, but t_c and t_c' do not. If we change the sign of the energy, the spectrum is the same for the (t_c, t_c') case and $(-t_c, -t_c')$; that is, the energy spectrum is reversed at $E = 0$.

[21]Change of the quantized Hall conductance in the two-dimensional graphite model was discussed by Haldane: F. D. M. Haldane, Phys. Rev. Lett. **61**, 2015 (1988).

[22]F. H. Claro and G. H. Wannier, Phys. Rev. B **19**, 6068 (1979).

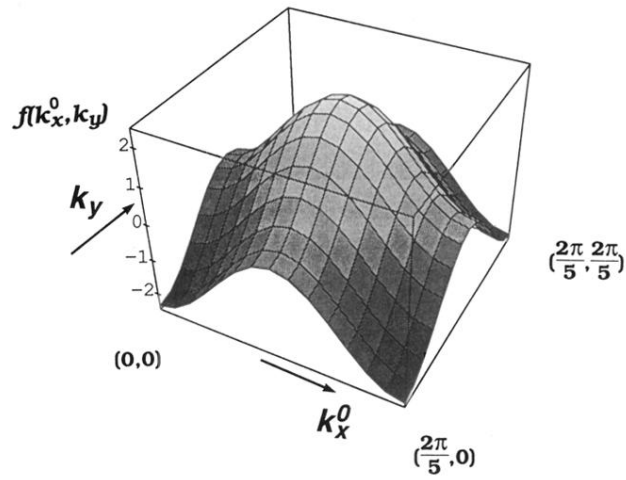[23]D. J. Thouless, Surf. Sci. **142**, 147 (1984).

FIG. 3. $f(k_x^0, k_y)$ for $p/q = \frac{2}{5}$ and $t_a = t_b = 1$, $t_c = t_c' = 0.3$. The magnetic Brillouin zone is q times larger in the k_y direction and $f(k_x, k_y)$ is periodic along this direction.
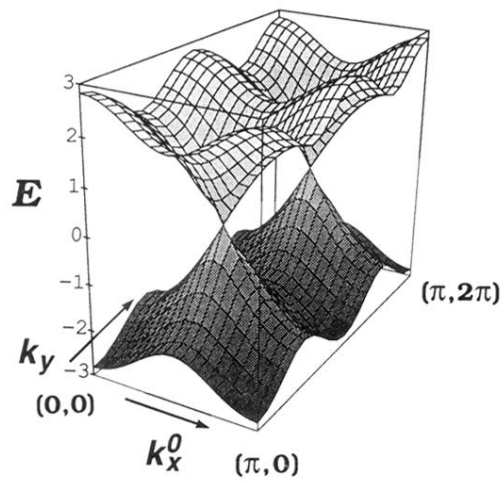
FIG. 6. The energy dispersion for $p/q = \frac{1}{2}$ and $t_a = t_b = 1$, $t_c = t_c' = 0.0$. The horizontal plane is the magnetic Brillouin zone. The existence of zero modes and the linear dispersion near these zero modes are seen.
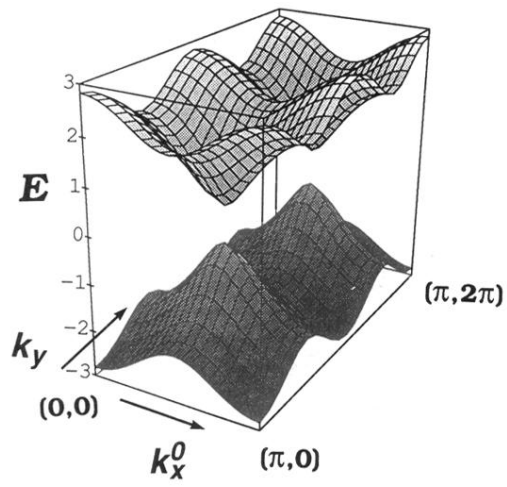
FIG. 7. Energy dispersion for $p/q = \frac{1}{2}$ and $t_a = t_b = 1$, $t_c = t_c' = 0.1$. The horizontal plane is the magnetic Brillouin zone. The degeneracy at the zero modes is removed.
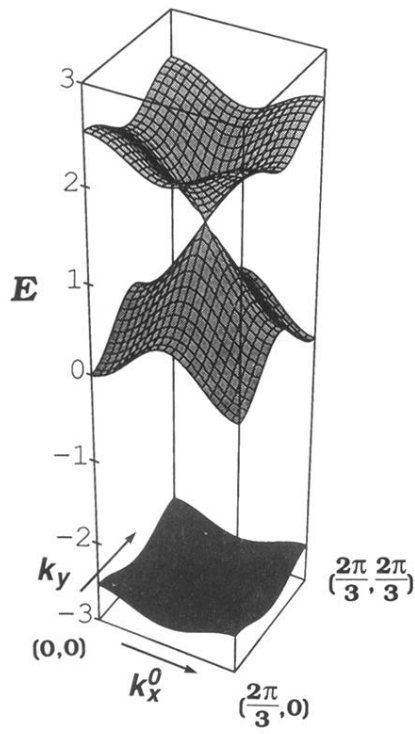
FIG. 9. Energy dispersion for $p/q = \frac{1}{3}$ and $t_a = t_b = 1$, $t_c = t_c' = 0.268$. The magnetic Brillouin zone is three times larger along the k_y direction, but the energy dispersion is periodic along this direction. This shows that there are degenerated modes and near these points dispersion is linear similar to the $\frac{1}{2}$ case in the NN model. The integers in the energy gaps are t_r.